The effects of Zn impurity on the properties of doped cuprates in the normal state

2004 J. Phys.: Condens. Matter 16 3703

(http://iopscience.iop.org/0953-8984/16/21/018)

INSTITUTE OF PHYSICS PUBLISHING JOURNAL OF PHYSICS: CONDENSED MATTER

J. Phys.: Condens. Matter **16** (2004) 3703–3710 PII: S0953-8984(04)75451-X

The effects of Zn impurity on the properties of doped cuprates in the normal state

Yun Song

Department of Physics, Beijing Normal University, Beijing 100875, People's Republic of China

Received 1 February 2004, in final form 23 March 2004
Published 14 May 2004
Online at stacks.iop.org/JPhysCM/16/3703
DOI: 10.1088/0953-8984/16/21/018

Abstract

We study the interplay of quantum impurity, and collective spinon and holon dynamics in Zn doped high-T_c cuprates in the normal state. The two-dimensional t–t'–J models with one Zn impurity and a small amount of Zn impurity are investigated within a numerical method based on the double-time Green function theory. We study the inhomogeneities of the holon density and antiferromagnetic correlation background in cases with different Zn concentrations, and obtain that doped holes tend to assemble around the Zn impurity with their mobility being reduced. Therefore a bound state of the holon is formed around the nonmagnetic Zn impurity with the effect helping Zn to introduce local antiferromagnetism around itself. The incommensurate peaks we obtained in the spin structure factor indicate that Zn impurities have effects on mixing the $q = (\pi, \pi)$ and 0 components in spin excitations.

The effects of divalent transition metal Zn substituted for Cu in the CuO_2 plane present much valuable information in understanding the mechanism of high temperature superconductors. Zn^{2+} has a closed d shell with spin $s = 0$, and acts as a very strong scattering centre. As a result, the spin configurations and the electronic structures around the nonmagnetic impurity Zn are strongly disrupted in both the normal state and superconducting state. Below T_c, there have been many experimental [1–5] and theoretical [6–10] investigations to discover how the d-wave superconductivity is destroyed and what the microscopic mechanism behind it is. As the normal state properties are more fundamental, some experimental [11–15] and theoretical [16–18] works have been done to study the effects of nonmagnetic impurity Zn on the properties of the normal state. It is believed that these studies are of great help in understanding the peculiar behaviours of the normal state. Moreover, they shed light on the recent striking issue of the normal state pseudogap [19, 20]. So far, there has been no clear picture of how the impurity interplays with the strong correlation background. It still remains unanswered why the Zn impurity produced very strong scatter and how the impurity band forms in real space.

In this paper, we perform numerical calculations to study the effects of Zn impurity on its surrounding Cu ions in the normal state. We want to find out how the Zn impurity

influences the hole distribution and the AF correlation background, which may bring about a better understanding of the fundamental relationship between spin and hole. We start from the two-dimensional (2D) t–t'–J model and use fermion-spin theory [21]. Fermion-spin theory is based on the charge–spin separation, in which the single occupied constraint of the t–t'–J model can be treated properly even in the mean field approximation. Within an improved Green function theory [22], we perform numerical calculations for cases with only one Zn impurity and a small amount of Zn impurity, and the effect of the Zn concentration on some properties of the normal state are discussed.

The essential physics of high-T_c cuprates is well described by the t–J model on a square lattice. Under the condition that Zn substitutes Cu in the CuO_2 plane, we can model the Zn impurity as a vacant site, which has no coupling with the surrounding Cu sites. We add the next-nearest-neighbour hopping term in our model to reproduce the realistic band structure, and start our study from the following Hamiltonian:

$$H = -t \sum_{\langle i,j\rangle\neq l,\sigma} (C^{\dagger}_{i\sigma} C_{j\sigma} + \text{h.c.}) - t' \sum_{\langle i,i'\rangle\neq l,\sigma} (C^{\dagger}_{i\sigma} C_{i'\sigma} + \text{h.c.}) - \mu \sum_{i,\sigma} C^{\dagger}_{i\sigma} C_{i\sigma} + J \sum_{\langle i,j\rangle\neq l} \mathbf{S}_i \cdot \mathbf{S}_j, \tag{1}$$

where $\langle i, j\rangle$ and $\langle i, i'\rangle$ mean the summations over nearest-neighbour (NN) and next-nearest-neighbour (NNN) pairs, respectively, and l represents the site occupied by the Zn impurity. In our model the direct hopping among a Zn impurity and its surrounding Cu sites is forbidden. In addition, to eliminate the doubly occupied sites of the Cu ion, we introduce the constraint $\sum_\sigma C^{\dagger}_{i\sigma} C_{i\sigma} \leqslant 1$ for each Cu site. Also we introduce $\sum_\sigma C^{\dagger}_{l\sigma} C_{l\sigma} = 2$ for the Zn^{2+} ion since it has a closed d shell. Therefore, the total number of electrons satisfies $\sum_{i\sigma} C^{\dagger}_{i\sigma} C_{i\sigma} = N - N_{\rm h} + N_{\rm Zn}$ with $N_{\rm h}$ and $N_{\rm Zn}$ representing the number of holes and Zn impurity, respectively. As the strong electron correlation manifests itself by the local constraint, the key issue is how to treat the constraint properly.

Here we study the t–t'–J model within the fermion-spin theory [21] based on the charge–spin separation. We introduce $C_{i\uparrow} = h^{\dagger}_i S^{-}_i$ and $C_{i\downarrow} = h^{\dagger}_i S^{+}_i$, where the spinless fermion operator h_i describes the charge (holon) degrees of freedom, while the pseudospin operator S_i describes the spin (spinon) degrees of freedom. Thus the low energy behaviour of the t–t'–J model (1) can be written as

$$H = -t \sum_{\langle i,j\rangle\neq l} (h_i h^{\dagger}_j + h_j h^{\dagger}_i)(S^{+}_i S^{-}_j + S^{-}_i S^{+}_j) - t' \sum_{\langle i,i'\rangle\neq l} (h_i h^{\dagger}_{i'} + h_{i'} h^{\dagger}_i)(S^{+}_i S^{-}_{i'} + S^{-}_i S^{+}_{i'}) + \mu \sum_{i\neq l} h^{\dagger}_i h_i + \sum_{\langle i,j\rangle\neq l} J^{\rm eff}_{i,j} \mathbf{S}_i \cdot \mathbf{S}_j, \tag{2}$$

where $J^{\rm eff}_{i,j} = [(1 - n^{\rm h}_i)(1 - n^{\rm h}_j) - \phi^2_{i,j}]J$ with $n^{\rm h}_i$ representing the hole concentration at site i and $\phi_{i,j} = \langle h^{\dagger}_i h_j\rangle$ being the order parameter of the holon. Here we also introduce spinon correlation functions $\chi_{ij} = \langle S^{-}_i S^{+}_j\rangle$ and $\chi^z_{ij} = \langle S^z_i S^z_j\rangle$.

We introduce three double-time Green functions

$$\begin{aligned} G_{\rm h}(i - j, \tau - \tau') &= -{\rm i}\theta(\tau - \tau')\langle [h_i(\tau); h^{+}_j(\tau')]\rangle \equiv \langle\langle h_i(\tau); h^{+}_j(\tau')\rangle\rangle \\ D_{\rm s}(i - j, \tau - \tau') &= -{\rm i}\theta(\tau - \tau')\langle [S^{+}_i; S^{-}_j(\tau')]\rangle \equiv \langle\langle S^{+}_i(\tau); S^{-}_j(\tau')\rangle\rangle \\ D^z_{\rm s}(i - j, \tau - \tau') &= -{\rm i}\theta(\tau - \tau')\langle [S^z_i; S^z_j(\tau')]\rangle \equiv \langle\langle S^z_i(\tau); S^z_j(\tau')\rangle\rangle, \end{aligned} \tag{3}$$

where $G_{\rm h}$ describes the behaviours of the holon, and $D_{\rm s}$ and $D^z_{\rm s}$ describe the behaviours of the spinon. Since the lattice translational invariance is not presented in cases with Zn impurities, we evaluate the equations of motion of the above Green functions in real space. The double-time Green function $\langle\langle A;\ B\rangle\rangle$ satisfies

$$\omega\langle\langle A;\ B\rangle\rangle_\omega = \langle [A, B]_{\mp}\rangle_\omega + \langle\langle [A,\ H];\ B\rangle\rangle_\omega, \tag{4}$$

thus we could obtain the equations of motion of $G_{\rm h}$

$$(\omega-\mu)G_{\rm h}(i-j)_\omega = 2t\sum_\eta \chi_{i,i+\eta}G_{\rm h}(i+\eta-j)_\omega + \delta(i-j) \times 2t'\sum_\tau \chi_{i,i+\tau}G_{\rm h}(i+\tau-j)_\omega. \tag{5}$$

We introduce $\widetilde{G_{\rm h}}$, a $N^2\times N^2$ elements matrix, to express the holon Green functions for a square lattice with $N\times N$ sites. We could rewrite equation (5) as

$$(\omega-\mu)\widetilde{G_{\rm h}} - \widetilde{h}\widetilde{G_{\rm h}} = \widetilde{I}, \tag{6}$$

where matrix $\widetilde{h}$ is decided by the NN and NNN spinon correlation functions, and $\widetilde{I}$ is an identity matrix.

Based on equations (3) and (4), we also obtain the equations of motion of spinon Green functions $D_{\rm s}$ and $D^z_{\rm s}$

$$\begin{aligned}\omega D_{\rm s}(i-j)_\omega &= 2\sum_\eta J^{\rm eff}_{i,i+\eta}\{\epsilon_{i,i+\eta}F_1(i,i+\eta;\ j)_\omega - F_1(i+\eta,i;\ j)_\omega\} \\ &\quad + 8t'\sum_\tau \phi_{i,i+\tau}F_1(i,i+\tau;\ j)_\omega \\ \omega D^z_{\rm s}(i-j)_\omega &= \sum_\eta J^{\rm eff}_{i,i+\eta}\epsilon_{i,i+\eta}\{F_2(i,i+\eta;\ j)_\omega - F_2(i+\eta,i;\ j)_\omega\} \\ &\quad + 4t'\sum_\tau \phi_{i,i+\tau}\{F_2(i,i+\tau;\ j)_\omega - F_2(i+\tau,i;\ j)_\omega\},\end{aligned} \tag{7}$$

where $\epsilon_{i,i+\eta} = 1+\frac{4t\phi_{i,i+\eta}}{J^{\rm eff}_{i,i+\eta}}$. F_1 and F_2 are the second-order spinon Green functions which are defined as

$$\begin{aligned}F_1(i,l;\ j)_\omega &= \langle\langle S^z_i S^+_l;\ S^-_j\rangle\rangle_\omega \\ F_2(i,l;\ j)_\omega &= \langle\langle S^+_i S^-_l;\ S^z_j\rangle\rangle_\omega.\end{aligned} \tag{8}$$

Going a step further, we establish the equations of motion of the second-order spinon Green functions

$$\begin{aligned}\omega F_1(i,l;\ j)_\omega &= 2\chi^z_{i,l}\delta(l-j) - \chi_{i,l}\delta(i-j) \\ &\quad + \left\langle\!\!\left\langle\left\{\sum_\eta[2J^{\rm eff}_{l,l+\eta}(\epsilon_{l,l+\eta}S^z_i S^z_l S^+_{l+\eta} - S^z_i S^z_{l+\eta}S^+_l) \right.\right.\right. \\ &\quad + J^{\rm eff}_{i,i+\eta}\epsilon_{i,i+\eta}(S^+_i S^-_{i+\eta}S^+_l - S^+_{i+\eta}S^-_i S^+_l)] \\ &\quad + 4t'\sum_\tau[\phi_{i,i+\tau}(S^+_i S^-_{i+\tau}S^+_l - S^+_{i+\tau}S^-_i S^+_l) \\ &\quad \left.\left.\left. + 2\phi_{l,l+\tau}S^z_i S^z_l S^+_{l+\tau}]\right\};\ S^-_j\right\rangle\!\!\right\rangle_\omega \\ \omega F_2(i,l;\ j)_\omega &= \chi_{i,l}\delta(l-j) - \chi_{i,l}\delta(i-j) \\ &\quad + \left\langle\!\!\left\langle\left\{\sum_\eta[2J^{\rm eff}_{l,l+\eta}(S^+_i S^-_l S^z_{l+\eta} - \epsilon_{l,l+\eta}S^+_i S^-_{l+\eta}S^z_l) \right.\right.\right. \\ &\quad + 2J^{\rm eff}_{i,i+\eta}(\epsilon_{i,i+\eta}S^+_{i+\eta}S^-_l S^z_i - S^+_i S^-_l S^z_{i+\eta})] \\ &\quad \left.\left.\left. + 8t'\sum_\tau[\phi_{i,i+\tau}S^+_{i+\tau}S^-_l S^z_i - \phi_{l,l+\tau}S^+_i S^-_{l+\tau}S^z_l]\right\};\ S^z_j\right\rangle\!\!\right\rangle_\omega.\end{aligned} \tag{9}$$

To the third-order spinon Green functions in the right-hand side of equation (9), we perform the improved decoupling scheme as described in [22], for example

$$\langle\langle S^z_i S^z_l S^+_{l+\eta};\ S^-_j\rangle\rangle \to \alpha_i\langle S^z_i S^z_l\rangle\alpha_l\langle\langle S^+_{l+\eta};\ S^-_j\rangle\rangle. \tag{10}$$

Therefore, the second-order spinon Green functions F_1 and F_2 can be expressed by the Green functions D_s and D_s^z as

$$\begin{aligned}\omega F_1(i,l;\ j)_\omega &= \Gamma_1^0 + \Gamma_1^1 D(i-j) + \sum_\eta \{\Gamma_1^2 D(i+\eta-j) + \Gamma_1^3 D(l+\eta-j)\} \\ &\quad + \Gamma_1^4 D(l-j) + \sum_\tau \{\Gamma_1^5 D(i+\tau-j) + \Gamma_1^6 D(l+\tau-j)\} \\ \omega F_2(i,l;\ j)_\omega &= \Gamma_2^0 + \Gamma_2^1 D^z(i-j) + \sum_\eta \{\Gamma_2^2 D^z(i+\eta-j) + \Gamma_2^3 D^z(l+\eta-j)\} \\ &\quad + \Gamma_2^4 D^z(l-j),\end{aligned} \tag{11}$$

where

$$\begin{aligned}\Gamma_1^0 &= 2\chi_{i,l}^z \delta(l-j) - \chi_{i,l}\delta(i-j), \\ \Gamma_1^1 &= \sum_\eta J_{i,i+\eta}^{\mathrm{eff}} \epsilon_{i,i+\eta}\alpha_{i+\eta}\chi_{i+\eta,l}\alpha_l + 4t' \sum_\tau \phi_{i,i+\tau}\alpha_{i+\tau}\chi_{i+\tau,l}\alpha_l, \\ \Gamma_1^2 &= -J_{i,i+\eta}^{\mathrm{eff}} \epsilon_{i,i+\eta}\alpha_i \chi_{i,l}\alpha_l, \\ \Gamma_1^3 &= 2J_{l,l+\eta}^{\mathrm{eff}} \epsilon_{l,l+\eta}\alpha_i \chi_{i,l}^z \alpha_l, \\ \Gamma_1^4 &= -2\sum_\eta J_{l,l+\eta}^{\mathrm{eff}} \alpha_i \chi_{i,l+\eta}^z \alpha_{l+\eta}, \\ \Gamma_1^5 &= -4t'\phi_{i,i+\tau}\alpha_i\chi_{i,l}\alpha_l, \\ \Gamma_1^6 &= 8t'\phi_{l,l+\tau}\alpha_i\chi_{i,l}^z\alpha_l, \\ \Gamma_2^0 &= \chi_{i,l}\delta(l-j) - \chi_{i,l}\delta(i-j), \\ \Gamma_2^1 &= 2\sum_\eta J_{i,i+\eta}^{\mathrm{eff}} \epsilon_{i,i+\eta}\beta_{i+\eta}\chi_{i+\eta,l}\beta_l + 8t' \sum_\tau \phi_{i,i+\tau}\beta_{i+\tau}\chi_{i+\tau,l}\beta_l, \\ \Gamma_2^2 &= -2J_{i,i+\eta}^{\mathrm{eff}} \beta_i \chi_{i,l}\beta_l, \\ \Gamma_2^3 &= 2J_{l,l+\eta}^{\mathrm{eff}} \beta_i \chi_{i,l}\beta_l\end{aligned}$$

and

$$\Gamma_2^4 = -2\sum_\eta J_{l,l+\eta}^{\mathrm{eff}} \epsilon_{l,l+\eta}\beta_i\chi_{i,l+\eta}\beta_{l+\eta} - 8t' \sum_\tau \phi_{l,l+\tau}\beta_i\chi_{i,l+\tau}\beta_{l+\tau}.$$

We also introduce two $N^2 \times N^2$ elements matrices $\widetilde{D}_s$ and $\widetilde{D}_s^z$ to express the spinon Green functions. Based on equations (7) and (11), we could obtain that

$$\begin{aligned}\omega^2\widetilde{D}_s - \widetilde{S}\widetilde{D}_s &= \widetilde{C}_s \\ \omega^2\widetilde{D}_s^z - \widetilde{S}^z\widetilde{D}_s^z &= \widetilde{C}_s^z,\end{aligned} \tag{12}$$

where matrices $\widetilde{S}$, $\widetilde{S}^z$, $\widetilde{C}_s$ and $\widetilde{C}_s^z$ are decided by the density of the holon n_i and the spin correlation functions.

We establish the self-consistent equations based on equations (6) and (12) to determine the correlation functions of the holon and the spinon, and also the vertex correction parameters. Under the periodic boundary conditions, we have performed numerical calculations for 16×16 and 20×20 lattices with different Zn concentrations. Based on the experimental results of BSCCO near optimal doping [1, 9], the parameters of the t–t'–J model are taken as $t/J = 2.5$ and $t'/t = -0.4$ in our calculations.

Firstly, we study the 20×20 lattice with only one Zn impurity in the optimally doping region ($\delta_h = 0.15$). The spacial distribution of holon density is calculated and our numerical results are shown in figure 1. We find that the holon density closest to the Zn impurity oscillates strongly, and the fluctuation diminishes rapidly away from the Zn impurity. The maximum

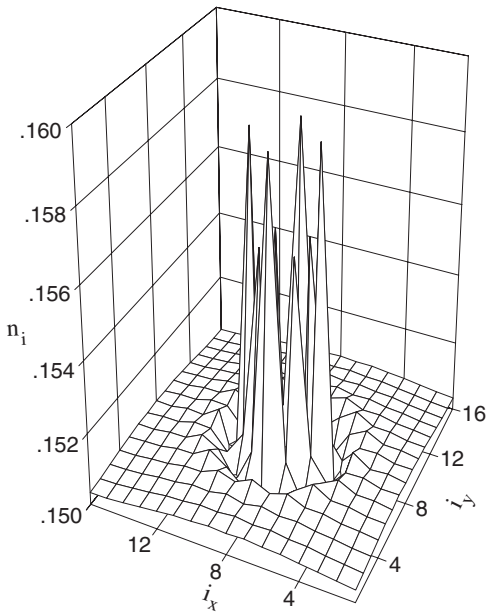

Figure 1. The distribution of holon density in a 20×20 lattice with only one Zn impurity.

density is obtained at sites two lattice distances away from the Zn impurity, and is about 15% higher than the minimum density. Our numerical results suggest that doped holes form a local region around the Zn impurity, whose size is about eight lattice cells, as shown in figure 1. We also obtain that the magnetic modification introduced by Zn is mainly in the vicinity of the Zn impurity. The NN correlation functions near the isolated nonmagnetic impurity in the undoped case have been discussed carefully in [22]. We have found that Zn impurity strongly modifies the spin excitations, especially the magnetic properties of the neighbour Cu. As a result, the AF correlation functions at the bonds close to the impurities are enhanced. In the optimally doped region, we also obtain that the Zn impurity enhances the NN AF correlation functions of spinons close to it. Moreover, the doped holes have the effect of strengthening the AF correlations near the Zn impurity. The ^{63}Cu NMR study of $YBa_2(Cu_{0.99}Zn_{0.01})_3O_{6.7}$ also finds that the AF correlations are enhanced, not destroyed, around Zn impurities [13]. Since the quantum fluctuation of spinons close to the nonmagnetic impurity is reduced obviously, we can divided the system into a strong AF correlation region and a weak AF correlation region. The tendency of doped holes to assemble around the Zn impurity could rationalize the anomalous charge localization effect, and the mobility of those holons close to the Zn impurity could also be reduced. Therefore, a bound state of the holon [23] is formed around the Zn impurity. The bound state of the impurity in the normal state has also been predicted by the self-consistent T matrix approach [18].

We also study the cases with several Zn impurities in the optimally doped regime, and find that the holes play different roles in the strong AF correlation regions and the weak AF correlation regions. We find that in different regions, that is in the strong AF correlation region and the weak AF correlation region, the hole plays different roles. Our numerical results show that the AF correlations of bonds far from the Zn impurity reduce remarkably as the hole is added into the systems. On the contrary, the bound state of the holon has the effect of enhancing the AF correlations around the Zn impurity, and helps Zn to introduce local antiferromagnetism

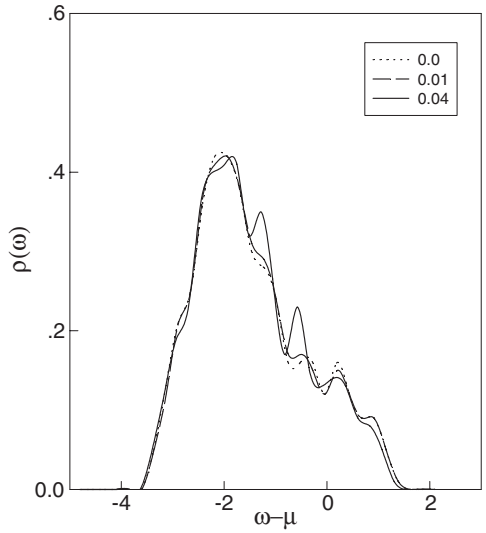

Figure 2. The density of states of the holon at $\delta_{\mathrm{Zn}} = 0.0$ (dotted curve), 0.01 (dashed curve) and 0.04 (solid curve).

around itself. As the Zn concentration increases, the CuO_2 plane becomes a inhomogeneous mixture of strong AF correlation regions and weak AF correlation regions, and the doped holes tend to assemble at the strong AF correlation regions.

We show the density of states of the holon in cases with several Zn impurities in figure 2. Jung *et al* [24] have examined some samples and prove that Zn is uniformly distributed. In some configurations when Zn is uniformly distributed, our calculations show that due to the strong coupling between impurity and the conduction band, the width of the holon band decreases as Zn concentration increases. We find that the inhomogeneity of the spinon background increases the density of states of the holon near the fermi surface, and a resonance peak of impurity states is found to get broader and stronger as the Zn concentration increases. Inelastic neutron scattering study for the optimal doped $La_{1.85}Sr_{0.15}Cu_{1-y}Zn_yO_4$ indicates that a new in-gap Zn impurity state is introduced at low temperature [25]. Nonmagnetic defect structures at the surface have also been found to create localized low-energy excitations in their immediate vicinity in $Bi_2Sr_2CaCu_2O_8$ by performing low-temperature tunnelling spectroscopy measurements with a scanning tunnelling microscope [4]. Our calculations show that the impurity state can survive above T_c, which is in agreement with theoretical prediction [18] as well.

To study the effect of the Zn impurity on the spin background around it, we introduce the spin structure factor

$$\mathbf{S}_i(\mathbf{k}) = \sum_j S_i^z S_j^z \mathrm{e}^{\mathbf{k}\cdot(\mathbf{i}-\mathbf{j})}. \tag{13}$$

Here i represents the Cu site around the Zn impurity. The Zn impurity is a scatter which has a strong effect on the AF correlation background [26]. As the Zn concentration increases, the CuO_2 plane becomes an inhomogeneous mixture of strong AF correlation regions and weak AF correlation regions. In figure 3, the numerical results of the NN Cu sites around the Zn impurity are shown for 16×16 lattices with different Zn concentrations. We obtain that, in the pure case and Zn lightly doped case ($\delta_{\mathrm{Zn}} \leqslant 0.01$), the spin excitations are dominated by a magnetic resonance peak located at $Q_{\mathrm{AF}} = (\pi, \pi)$. As the Zn concentration increases, this

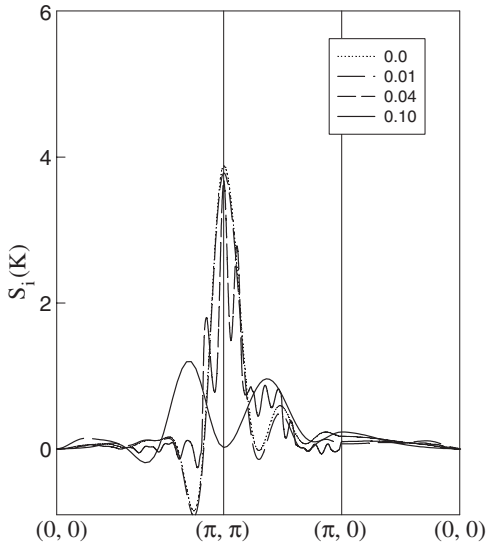

Figure 3. The spin structure factor of the nearest neighbour Cu sites around the Zn impurity for 16×16 lattices with different Zn concentrations.

peak decreases and there appear two second-high incommensurate peaks as shown in figure 3, which result from the mixing of $q = (\pi, \pi)$, $(\pi, 0)$ and 0 components in spin excitations introduced by the strong impurity scattering. In Bulut's study of susceptibility of Zn doped high-T_c superconductors, similar behaviours are also obtained [17]. In addition, we find that the distances of the incommensurate peaks from $q = (\pi, \pi)$ increase with doping, and these peaks become broad and weak in amplitude with increasing of Zn concentration. Meanwhile, as a result of increasing the disorder introduced by the Zn substitution on the Cu sites, the peak at $q = (\pi, \pi)$ decreases gradually as the Zn concentration increases, and disappears when $\delta_{Zn} \geqslant 0.1$. Thus the result is consistent with experimental results of Zn-doped high-T_c cuprates [11].

In summary, we have studied the interplay between quantum impurities, and collective spinon and holon dynamics in Zn-doped cuprate in the normal state. Within a numerical method based on the Green function theory, the inhomogeneities of the holon density distribution and the antiferromagnetic correlation background in the two-dimensional t–t'–J model with Zn impurities are investigated. We obtain the real space shape of the bound state of the holon surrounding the nonmagnetic Zn impurity. We also find that the doped holes help Zn to introduce local antiferromagnetism around itself. In the cases with a small amount of Zn impurity, the influence of the Zn impurity on the antiferromagnetic correlation background is studied. The appearance of incommensurate peaks in the spin structure factor indicates that the Zn impurity is a strong scatter centre, which has an effect on mixing the $q = (\pi, \pi)$, $(\pi, 0)$ and 0 components in spin excitations.

Acknowledgments

The authors would like to thank Professor Feng for helpful discussions. This work was supported by the grant from Beijing Normal University.

References

[1] Pan S H, Hudson E W, Lang K M, Eisaki H, Uchida S and Davis J C 2000 *Nature* **403** 746
[2] Sidis Y, Bourges P, Fong H F, Keimer B, Regnault L P, Bossy J, Ivanov A, Hennion B, Gautier-Picard P, Collin G, Millius D L and Aksay I A 2000 *Phys. Rev. Lett.* **84** 5900
[3] Hudson E W, Pan S H, Gupta A K, Ng K-W and Davis J C 1999 *Science* **285** 88
[4] Yazdani A, Howald C M, Lutz C P, Kapitulnik A and Eigler D M 1999 *Phys. Rev. Lett.* **83** 176
[5] Mahajan A V, Alloul H, Collin G and Marucco J F 1994 *Phys. Rev. Lett.* **72** 3100
[6] Polkovnikov A, Sachdev S and Vojta M 2001 *Phys. Rev. Lett.* **86** 296
[7] Balatsky A V 2000 *Nature* **403** 717
Salkola M I, Balatsky A V and Scalapino D J 1996 *Phys. Rev. Lett.* **77** 1841
Balatsky A V, Salkola M I and Rosengren A 1995 *Phys. Rev.* B **51** 15547
[8] Zhu J-X, Lee T K, Ting C S and Hu C-R 2000 *Phys. Rev.* B **61** 8667
[9] Tsuchiura H, Tanaka Y, Ogata M and Kashiwaya S 2000 *Phys. Rev. Lett.* **84** 3165
Tsuchiura H, Tanaka Y, Ogata M and Kashiwaya S 1999 *J. Phys. Soc. Japan* **68** 2510
[10] Xiang T, Su Y H, Panagopoulos C, Su Z B and Yu L 2002 *Phys. Rev.* B **66** 174504
[11] Alloul H, Mendels P, Casalta H, Marucco J F and Arabski J 1991 *Phys. Rev. Lett.* **67** 3140
[12] Bobroff J, Alloul H, Yoshinari Y, Keren A, Mendels P, Blanchard N, Collin G and Marucco J-F 1997 *Phys. Rev. Lett.* **79** 2117
Bobroff J, MacFarlane W A, Alloul H, Mendels P, Blanchard N, Collin G and Marucco J-F 1999 *Phys. Rev. Lett.* **83** 4381
[13] Julien M-H, Fehér T, Horvatic M, Berthier C, Bakharev O N, Ségransan P, Collin G and Marucco J-F 2000 *Phys. Rev. Lett.* **84** 3422
[14] MacFarlane W A, Bobroff J, Alloul H, Mendels P, Blanchard N, Collin G and Marucco J-F 2000 *Phys. Rev. Lett.* **85** 1108
[15] Yamagata H, Miyamoto H, Nakamura K, Matsumura M and Itoh Y 2003 *Preprint* cond-mat/0304477
[16] Nagaosa N and Lee P A 1997 *Phys. Rev. Lett.* **79** 3755
[17] Bulut N 2000 *Phys. Rev.* B **61** 9051
[18] Kruis H V, Martin I and Balatsky A V 2001 *Phys. Rev.* B **64** 054501
[19] Tallon J L, Bernhard C, Williams G V M and Loram J W 1997 *Phys. Rev. Lett.* **79** 5294
Tallon J L 1998 *Phys. Rev.* B **58** 5956
[20] Chattopadhyay B, Bandyopadhyay B, Poddar A, Mandal P, Das A N and Ghosh B 2000 *Physica* C **331** 38
[21] Feng S, Su Z B and Yu L 1994 *Phys. Rev.* B **49** 2368
Feng S, Su Z B and Yu L 1993 *Mod. Phys. Lett.* B **7** 1013
Feng S and Song Y 1997 *Phys. Rev.* B **55** 642
[22] Song Y, Lin H Q and Shen J-L 1998 *Phys. Rev.* B **58** 9166
Song Y, Lin H Q and Sandvik A W 2000 *J. Phys.: Condens. Matter* **12** 5275
[23] Poilblanc D, Scalapino D J and Hanke W 1994 *Phys. Rev. Lett.* **72** 884
Ziegler W, Poilblanc D, Preuss R, Hanke W and Scalapino D J 1996 *Phys. Rev.* B **53** 8704
[24] Jung C U, Kim J Y, Park M-S, Kim M-S, Kim H-J, Lee S Y and Lee S-I 2002 *Phys. Rev.* B **65** 172501
[25] Kimura H, Kofu M, Matsumoto Y and Hirota K 2002 *Preprint* cond-mat/0209428
[26] Vajk O P, Mang P K, Greven M, Gehring P M and Lynn J W 2002 *Science* **295** 1691